Available online at www.sciencedirect.com
ScienceDirect
Metabolism Clinical and Experimental 59 (2010) 1680 – 1690
Metabolism
Clinical and Experimental
www.metabolismjournal.com

Skeletal muscle catabolism in trinitrobenzene sulfonic acid–induced murine colitis

Frances Puleo[a], Katia Meirelles[a], Maithili Navaratnarajah[a], Leo Fitzpatrick[b], Margaret L. Shumate[a], Robert N. Cooney[a,c,1], Charles H. Lang[a,c,*]

[a]*Department of Surgery, Penn State College of Medicine, Hershey, PA 17033, USA*
[b]*Department of Pharmacology, Penn State College of Medicine, Hershey, PA 17033, USA*
[c]*Department of Cellular and Molecular Physiology, Penn State College of Medicine, Hershey, PA 17033, USA*

Received 19 November 2009; accepted 30 March 2010

Abstract

The present study determined whether the muscle atrophy produced by colitis is associated with altered rates of muscle protein synthesis or degradation, as well as the potential role of the local (eg, muscle) insulin-like growth factor (IGF) system and muscle-specific ubiquitin E3 ligases atrogin-1 and MuRF1 in mediating altered muscle protein balance. Colitis was induced in C57BL/6 mice by intrarectal administration of trinitrobenzene sulfonic acid (TNBS), and blood and tissues were collected on day 10. Mice with inflammatory bowel disease demonstrated reduced skeletal muscle mass and protein content, whereas colonic segment weight and gross damage score were both increased in mice with colitis, compared with time-matched control values. There was no change in muscle protein synthesis in mice with inflammatory bowel disease; but there was an increased protein breakdown (45%), proteasome activity (85%), and messenger RNA (mRNA) expression for atrogin-1 and MuRF1 (200%-300%) in muscle. These changes were associated with a reduction in liver (but not muscle) IGF-I mRNA as well as a reduction in both total and free IGF-I in the blood. Colitis decreased the hepatic content of IGF binding protein (IGFBP)–3 mRNA by 40% and increased IGFBP-1 mRNA by 100%. In contrast, colitis did alter IGFBP mRNAs in muscle. The tumor necrosis factor–α, interleukin-6, and nitric oxide synthase 2 mRNA content of both liver and skeletal muscle was increased in TNBS-treated mice; and plasma tumor necrosis factor–α and interleukin-6 concentrations were also elevated. These data suggest that TNBS-induced colitis is independent of a change in muscle protein synthesis but dependent on stimulation of protein degradation via increased expression of muscle-specific atrogenes, which may be mediated in part by the reduction in circulating concentration of IGF-I and the concomitant increase in inflammatory mediators observed in the blood and muscle per se.

1. Introduction

Impaired linear growth, osteopenia, and reduction in lean body mass (LBM) are commonly seen in children with inflammatory bowel disease (IBD), such as Crohn disease and ulcerative colitis [1,2]. The IBD-related growth failure and decreased muscle mass have been attributed to a variety of mechanisms including decreased nutrient intake, malabsorption of ingested nutrients, increased metabolic rate, and the inhibitory effects of inflammation on the growth hormone (GH)/insulin-like growth factor (IGF)–I axis [3-5]. Normally, circulating GH binds to transmembrane GH receptors and activates the transcription of IGF-I in liver and other tissues [6]. The synthesis of circulating IGF-I by liver and its local production by bone and muscle stimulate the proliferation of chondrocytes and osteoblasts in the epiphyseal growth plate of long bones, resulting in linear growth [7]. Insulin-like growth factor–I also regulates muscle mass by enhancing protein synthesis and slowing the rate of proteolysis [8,9]. Conversely, both plasma IGF-I and muscle IGF-I are decreased in response to diverse inflammatory insults that accelerate the loss of muscle protein [9]. The inflammatory cytokines tumor necrosis factor (TNF)–α and interleukin (IL)-6 in particular are elevated during IBD [10-12]. Such increases produce hepatic GH resistance and decrease circulating IGF-I that ultimately impairs growth and accretion

* Corresponding author. Department of Cellular and Molecular Physiology, H166, Penn State College of Medicine, Hershey, PA 17033, USA. Tel.: +1 717 531 5538; fax: +1 717 531 7667.
E-mail address: clang@psu.edu (C.H. Lang).
[1] RN Cooney, current address: Upstate Medical University, Department of Surgery, Syracuse, NY 13210.

0026-0495/$ – see front matter © 2010 Elsevier Inc. All rights reserved.
doi:10.1016/j.metabol.2010.03.021

of LBM [13]. However, tissue IGF-I availability is complex and regulated not only by the concentration of IGF-I per se but also by changes in either the amount or type(s) of various IGF binding proteins (IGFBPs) produced by the liver or target organ (eg, muscle) [14]. For example, elevations in IGFBP-1 effectively inhibit the ability of IGF-I to stimulate muscle protein synthesis [15,16]. Although changes in the circulating concentration of several IGFBPs have been reported in patients with IBD [17,18], no comparable information is available in rodent models of IBD; and whether the synthesis of the various IGFBPs differs between liver and muscle in this inflammatory condition is unknown.

Muscle catabolism is multifactorial, being caused by both reduced protein synthesis and increased protein degradation. Previous studies that have directly assessed muscle protein synthesis have yielded conflicting results, with muscle protein synthesis being decreased in rats receiving dextran sulfate sodium [19] and increased in HLA-B27 rats that develop spontaneous IBD [20]. Furthermore, there are essentially no data on muscle protein degradation in IBD and colitis. Current evidence indicates that the ubiquitin (Ub)-proteasome–dependent pathway is the most prevalent mechanism regulating muscle proteolysis during systemic inflammation [21]. This pathway identifies specific proteins for degradation through a series of enzymatic reactions that attach a polyubiquitin chain to the target peptide, resulting in its proteasomal degradation [22]. The targeting process involves the coordinating activity of E1 (Ub-activating), E2 (Ub-conjugating), and E3 (Ub-ligating) enzymes. The Ub-ligating enzymes muscle RING finger 1 (MuRF1) and muscle atrophy F-box (atrogin-1) are muscle-specific enzymes that appear to be causally related to muscle protein breakdown observed in a number of catabolic conditions including denervation, sepsis, diabetes, fasting, and excessive production of glucocorticoids and inflammatory cytokines [12,23-25]. To further emphasize the significance of these enzymes, MuRF1 and atrogin-1 are often referred to as *atrophy-related* or *atrogenes*. The interaction of IGF-I and atrogenes in controlling muscle integrity is evidenced by the ability of this anabolic hormone to decrease muscle atrogene expression and thereby limit protein degradation by inhibiting proteolytic pathways [24,26-28]. Therefore, the purpose of the present study was to determine whether the muscle atrophy produced by trinitrobenzene sulfonic acid (TNBS)–induced colitis is associated with altered rates of muscle protein synthesis or degradation, as well as the potential role of the local (eg, muscle) IGF system and muscle-specific Ub E3 ligases atrogin-1 and MuRF1 in mediating altered muscle protein balance.

2. Materials and methods

2.1. Animal model of colitis and experimental protocol

Male C57Bl/6 mice (approximately 50 days of age; Charles River Breeding Laboratories, Cambridge, MA) were used in all studies and were housed in a light-controlled room under constant environmental conditions. Standard rodent chow was provided ad libitum. All experiments were approved by the Institutional Animal Care and Use Committee of The Pennsylvania State University College of Medicine and adhere to the National Institutes of Health guidelines for the use of experimental animals. Mice were anesthetized with an intraperitoneal injection of ketamine (136 mg/kg) and xylazine (9.6 mg/kg) followed by the intrarectal administration of 2,4,6-TNBS (40 μg/g in 50% ethanol; 100-μL volume) or an equal volume of 50% ethanol on day 0 [29]. The mice underwent a second administration of TNBS or ethanol on day 7 of the study to reactivate the hapten-mediated colitis. Animals were followed for a total of 10 days, were weighed every day, and were provided rodent chow ad libitum. Our preliminary studies indicated that 2 injections of TNBS were necessary to develop a sustained inflammatory condition capable of producing a detectable decrease in muscle mass.

Specifically, mice were killed 3 days after the second TNBS injection (eg, 10 days from first injection) because this time point represented the peak of the inflammatory state. This animal model is characterized by transmural and chronic colonic inflammation similar to that observed in patients with Crohn disease [4]. Although we recognize that ketamine anesthesia can alter muscle protein metabolism [30], control animals received the same dose of anesthetic as those administered TNBS. Body weight was determined every other day, and the overall length was measured from the tip of the nose to the tail on study days 0 and 10. On day 10, the mice were anesthetized; and then blood and tissues were collected. An intracardiac puncture was performed, and blood was collected in heparinized tubes. The plasma was removed and stored at −20°C for later analyses. The gastrocnemius-plantaris complex was removed together with a portion of liver; tissues were frozen to the temperature of liquid nitrogen, weighed, and then stored at −80°C. The colon from each mouse was weighed and graded on degree of inflammation. The colonic damage was assessed on a scale of 0 to 10 using the colonic macroscopic scoring system described in Table 1.

Table 1
Colonic macroscopic scoring system

Score	Parameter
0	No damage
1	Hyperemia without ulcers
2	Hyperemia and bowel thickening, without ulcers
3	1 site of ulceration without bowel thickening
4	2 or more sites of ulceration or inflammation
5	>2 sites of damage or 1 site 0.5 cm
6-10	Damage of at least 1 cm, with score increasing by 1 for each additional 0.5 cm of damage

Each colon was weighed and graded on degree of inflammation with colonic damage assessed on a scale of 0 to 10.

2.2. Skeletal muscle protein metabolism

Protein synthesis was determined using the flooding-dose technique as originally described by Garlick et al [31] and modified by our laboratory [16,32,33]. Mice were fasted for 4 hours and then injected intraperitoneally with [3H]-L-phenylalanine (Phe; 150 mmol/L, 30 μCi/mL; 1 mL/100 g body weight). An arterial blood sample was collected 15 minutes later for the determination of phenylalanine concentration and radioactivity, and the rate of protein synthesis was calculated using the specific radioactivity of the plasma Phe as the precursor pool.

Immediately after the removal of the blood, the gastrocnemius was excised, frozen between liquid nitrogen–cooled aluminum blocks, and stored at −80°C. Tissue protein concentration was determined using the bicinchoninic acid procedure (Pierce Chemical, Rockford, IL) with crystalline bovine serum albumin as a standard.

As tyrosine is neither synthesized nor degraded in muscle, we determined the rate of protein degradation in plantaris muscle by assessing the tyrosine released into the incubation medium. The plantaris muscle was secured to a plastic support to maintain resting length during incubation, and the incubation composition and conditions were exactly as previously described [34]. Tyrosine in the medium was assayed fluorometrically [35].

2.3. Proteasome activity

In vitro proteasome activity was assessed by quantifying the chymotryptic-like peptidase activity in gastrocnemius muscle. Muscle was homogenized in buffer containing 50 μmol/L Tris-HCl (pH 7.4), 5 mmol/L $MgCl_2$, 250 mmol/L sucrose, 2 mmol/L adenosine triphosphate, and 1 mmol/L dithiothreitol. The homogenate was first centrifuged at 4000*g* (5 minutes) and clarified by sequential centrifugation steps (10 000*g* for 20 minutes followed by 100 000*g* for 5 hours) to isolate the 20S and 26S proteasomes, as previously described [36,37]. After resuspension, proteasome chymotryptic-like activity was determined using a fluorometer (Molecular Devices SpectraMax Gemini EM, Toronto, Canada) to measure the release of 7-amino-4-methylcoumarin from the fluorogenic peptide substrate LLVY-AMC (Chemicon International, Temecula, CA).

2.4. Ribonuclease protection assays

Primer selection for mouse genes of interest was determined with the help of Genefisher software, and template production was performed as previously described [24]. Primers were synthesized (IDT, Coralville, IA) with restriction sites for *Eco*RI or *Kpn*I at the 5′ end and with 3 extra bases at the extreme 5′ end. Primer sequences for one template contained IGF-I, atrogin-1, MuRF1, and E3α1, which have been previously published by our laboratory [25]. Riboprobes for cytokine studies were synthesized from custom multiprobe mouse template sets containing probes for IL-6, TNF-α, IL-1α, and nitric oxide synthase (NOS) 2 as previously described [38,39]. Quantitation of the messenger RNA (mRNA) content for IGFBP-1, -2, -3, -4, -5, and -6 as well as the acid-labile subunit (ALS) was as described [40]. Each template contained actin, L32, and/or glyceraldehyde-3-phosphate dehydrogenase as loading controls. In general, polymerase chain reaction (PCR) was conducted using HotStarTaq DNA Polymerase (Qiagen, Valencia, CA); and total RNA was reverse-transcribed with Superscript First-Strand Synthesis System for RT-PCR (Invitrogen, Carlsbad, CA). Polymerase chain reaction products were phenol: chloroform extracted, ethanol precipitated, and sequentially digested with *Kpn*I and *Eco*RI (Promega, Madison, WI). Digested products were gel purified, reextracted, and cloned into *Kpn*I/*Eco*RI-digested pBluescript II SK+ (Stratagene, La Jolla, CA). Plasmid DNA was isolated with both QIAprepR Spin Miniprep and Plasmid Maxi Kits (Qiagen). Plasmids with inserts were verified by sequencing in the Pennsylvania State College of Medicine Core Facility. Final constructs were linearized with *Eco*RI, gel purified, and quantitated spectrophotometrically.

Total RNA was extracted from cells using TRI Reagent (Molecular Research Center, Cincinnati, OH). Tissue mRNA content was determined by ribonuclease protection assay (RPA) as described [15,25,39]. Briefly, a 2-μL aliquot of template was prepared using T7 Polymerase with buffer (Fermentas, Hanover, MD), NTPs and tRNA (Sigma-Aldrich), RNaisin and DNase (Promega, Madison, WI), and 32P-UTP (Amersham Biosciences, Piscataway, NJ). Unless otherwise noted, the RPA procedure including labeling conditions, component concentrations, sample preparation, and gel electrophoresis was as published (BD Pharmingen, San Diego, CA). Hybridization buffer was 80% formamide and 20% stock buffer (200 mmol/L PIPES [pH 6.4], 2 mol/L NaCl, and 5 mmol/L EDTA). Hybridization proceeded overnight at 56°C in a dry bath incubator (Fisher Scientific, Pittsburgh, PA). Samples were treated with RNase A+ T_1 (Sigma) in 1× RNase buffer (10 mmol/L Tris-HCl [pH 7.5], 5 mmol/L EDTA, and 300 mmol/L NaCl) followed by Proteinase K in 1× Proteinase K buffer (50 mmol/L Tris [pH 8.0], 1 mmol/L EDTA, 1% Tween-20). After ethanol precipitation, samples were resuspended in loading buffer (98% formamide [vol/vol], 0.05% xylene cyanol [wt/vol], 0.05% bromophenol blue [wt/vol], and 10 mmol/L EDTA). Polyacrylamide gels were run in an S3S Sequencing System (Owl Separation Systems, Portsmouth, NH), transferred to chromatography paper, and dried (FB GD 45 Gel Dryer, Fisher Scientific). Gels were exposed to a PhosphorImager screen (Molecular Dynamics, Sunnyvale, CA). Data were visualized and analyzed using ImageQuant software (Version 5.2, Molecular Dynamics). Signal densities within the linear range were normalized to densities for actin, L32, and/or glyceraldehyde-3-phosphate dehydrogenase mRNA.

2.5. Western blot analysis

The tissue preparation was the same as described by our laboratories [32,33,41-43]. Muscle was homogenized in ice-

cold homogenization buffer (pH 7.4) composed of (in millimoles per liter): 20 HEPES, 2 EGTA, 50 NaF, 100 KCl, 0.2 EDTA, 50 β-glycerophosphate, 1 dithiothreitol, 0.1 phenylmethylsulfonyl fluoride, 1 benzamidine, 0.5 sodium vanadate, plus 1 protease inhibitor cocktail tablet from Roche (Mannheim, Germany), and clarified by centrifugation. The samples were subjected to sodium dodecyl sulfate polyacrylamide gel electrophoresis, and the proteins were electrophoretically transferred to polyvinylidene difluoride membranes. The blots were incubated with either primary antibodies to total and phosphorylated (Thr37/46) eukaryotic initiation factor 4E binding protein–1 (4E-BP1; Bethyl Laboratories, Montgomery, TX) or total and phosphorylated (Thr389; Cell Signaling, Beverly, MA) ribosomal protein S6 kinase–1 (S6K1). Blots were washed with TBS-T (1× TBS including 0.1% Tween-20) and incubated with secondary antibody (horseradish peroxidase–conjugated goat anti-mouse or goat anti-rabbit) immunoglobulin G. Blots were developed with enhanced chemiluminescence Western blotting reagents (Amersham) and exposed to x-ray film in a cassette equipped with a DuPont Lightning Plus intensifying screen (Sigma-Aldrich). After development, the film was scanned (Microtek ScanMaker IV; Cerritos, CA) and analyzed using National Institutes of Health (Bethesda, MD) Image 1.6 software.

2.6. Plasma IGF-I, insulin, and cytokine determinations

Total plasma IGF-I was measured using a mouse/rat IGF-I radioimmunoassay kit (Diagnostic Systems Laboratories, Webster, TX). The plasma concentration of free (or readily dissociable) IGF-I was determined by centrifugal ultrafiltration exactly as previously described [15]. The plasma insulin concentration was determined by radioimmunoassay (Linco Research, St Louis, MO). Tumor necrosis factor–α and IL-6 in plasma were quantified by commercially available enzyme-linked immunosorbent assays (R&D Systems, Minneapolis, MN).

2.7. Statistical analysis

Data are presented as mean ± SE, and the exact sample size is indicated in the figure and table legends. Statistical evaluation of the data was performed by 2-tailed *t* test using Instat GraphPad 5.02 (San Diego, CA). Differences among groups were considered significant at $P < .05$. Differences between groups with a P value > .05 but < .01 are referred to as *trends*, whereas between-group differences with a $P > .10$ were considered not statistically significant.

3. Results

3.1. Food intake, body weight, muscle weight, linear growth, and severity of colitis

Food consumption was reduced for 1 to 2 days after each injection of TNBS compared with time-matched vehicle-treated control values (day 1: control = 3.7 ± 0.2 vs TNBS = 2.1 ± 0.4 g/d, day 2: control = 4.3 ± 0.3 vs TNBS = 3.4 ± 0.3 g/d, and day 7: control = 4.1 ± 0.3 vs TNBS = 2.0 ± 0.4 g/d; $P < .05$). However, food intake did not differ between control and TNBS-treated mice on days 3 to 6 (control = 3.9 ± 0.3 vs TNBS = 3.6 ± 0.4 g/d, $P > .10$) or on days 8 to 10 (control = 4.3 ± 0.3 vs TNBS = 4.1 ± 0.3 g/d, $P > .10$). The final body weight (control = 23.1 ± 0.3 vs TNBS = 22.6 ± 0.3 g) and rate of body weight gain (control = 0.50 ± 0.04 vs TNBS = 0.42 ± 0.04 g/d)

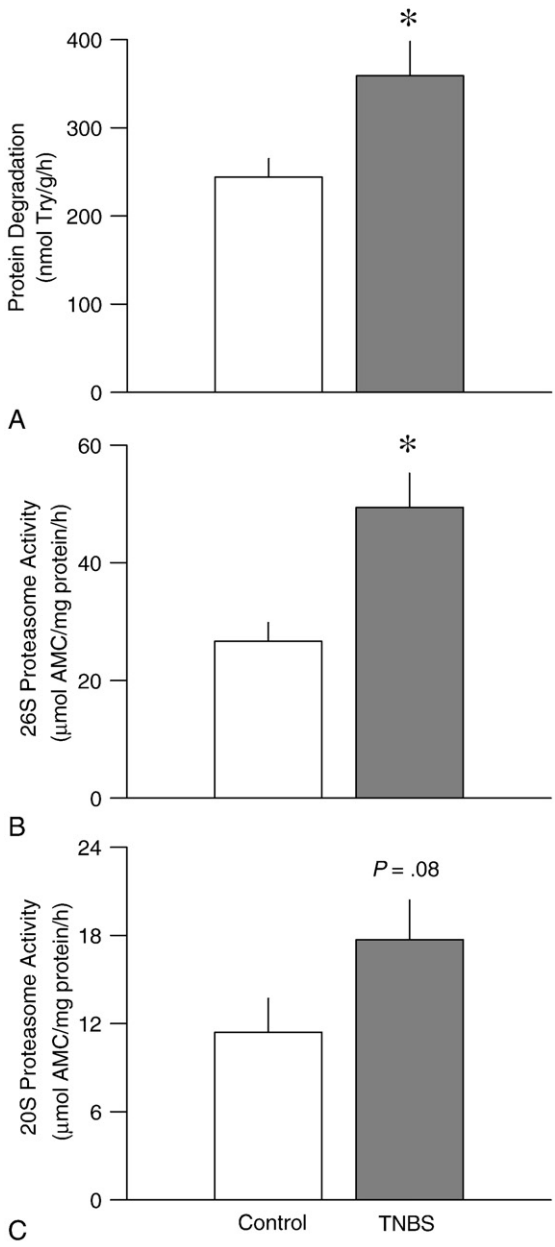

Fig. 1. Effect of TNBS-induced colitis on in vitro–determined rates of muscle protein breakdown and proteasome activity. A, Protein degradation in plantaris determined by tyrosine (Try) release into medium. B and C, Activity of the 26S and 20S proteasome, respectively. Values are means ± SEM; n = 8 to 10 per group for protein degradation and 6 per group for proteasome activity. *$P < .05$ compared with time-matched control values.

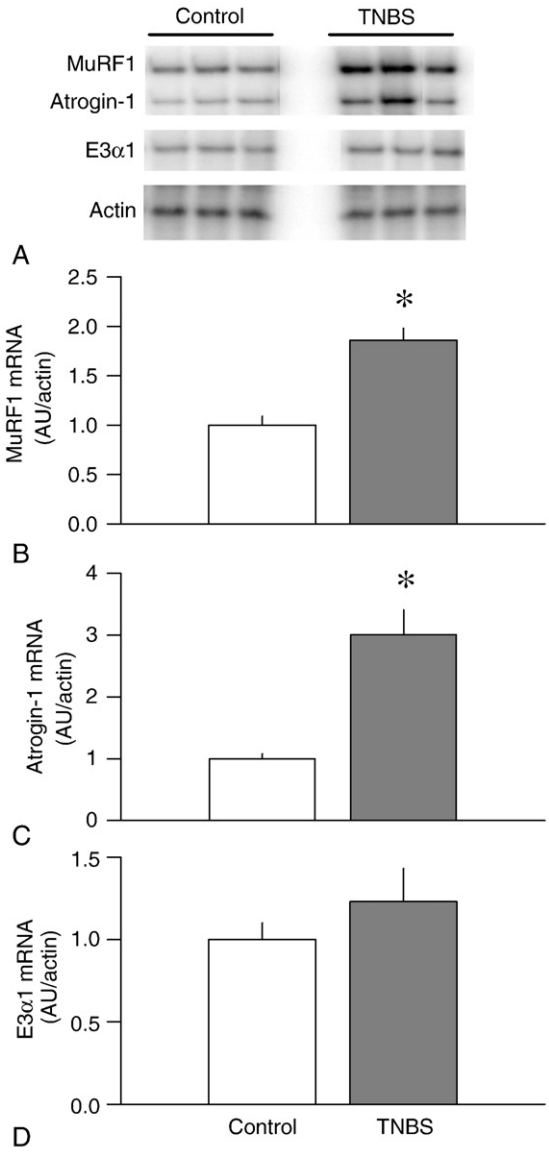

Fig. 2. Effect of TNBS-induced colitis on MuRF1, atrogin-1, and E3αI mRNA content in skeletal muscle. A, Representative autoradiographs of E3 ligases and actin (loading control). B to D, Bar graphs represent means ± SEM of n = 9 to 11; data were normalized to actin and expressed as arbitrary densitometry units (AU)/actin. Data from control mice were arbitrarily set at 1.0 AU. *$P < .05$ compared with time-matched control values.

did not differ between TNBS-treated and control mice. The increment in linear growth of mice with colitis tended to be reduced compared with control values (controls = 3.7 ± 0.4 vs TNBS = 2.4 ± 0.04 mm/10 d, $P = .07$).

However, the wet weight of the gastrocnemius-plantaris complex was significantly reduced by 13% in mice with colitis compared with control values (control = 219 ± 8 vs 188 ± 8 mg, $P < .05$). In contrast, the wet weight of the heart did not differ between groups (control = 95 ± 4 vs TNBS = 92 ± 3 mg). Colonic weight of TNBS-treated mice was increased compared with control values (control = 107 ± 4 vs 136 ± 7 mg/cm^3, $P < .05$). Likewise, the severity of disease, based on the gross damage score, was greater in the mice with colitis (control = 0.7 ± 0.2 vs 3.3 ± 0.4, $P < .05$).

3.2. Muscle protein concentration, synthesis, and degradation

Skeletal muscle protein concentration was reduced by 11% in mice with colitis compared with time-matched control values (control = 167. 4 ± 6.6 vs TNBS = 148.2 ± 7.1 mg protein per gram wet weight, $P < .05$, n = 8 per group). However, in vivo determined muscle protein synthesis did not differ between control and TNBS-treated mice (0.85 ± 0.05 vs 0.83 ± 0.04 nmol Phe incorporated per hour per milligram, respectively; n = 8 per group). The mammalian target of rapamycin is a Ser/Thr kinase that regulates muscle protein synthesis by integrating various nutrient and growth factor signals [44]; and this regulation is largely achieved by the phosphorylation of 2 downstream targets, 4E-BP1 and S6K1. Western blot analysis of muscle from TNBS-treated mice and

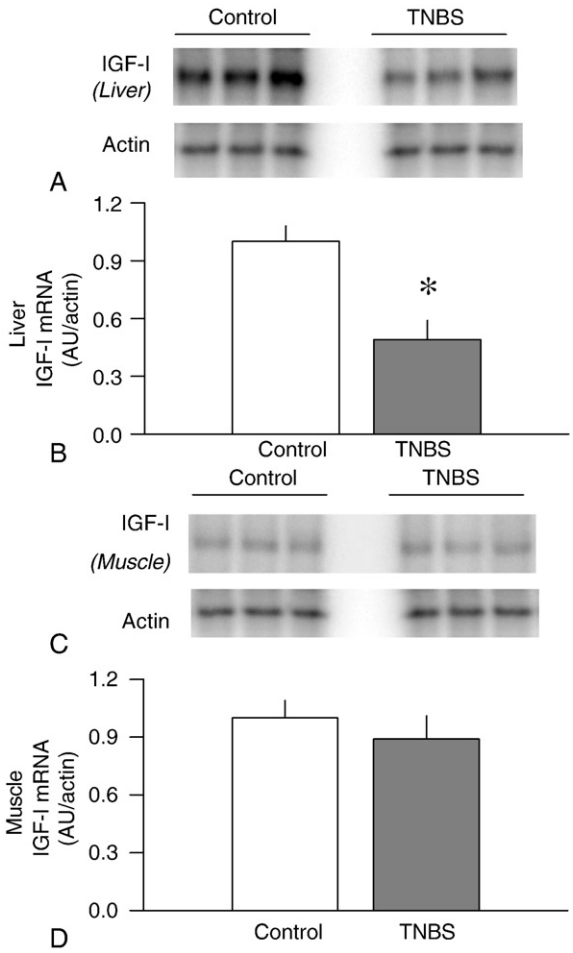

Fig. 3. Effect of TNBS-induced colitis on the IGF-I mRNA content of liver and skeletal muscle. A and C, Representative autoradiographs of IGF-I mRNA in liver and muscle (gastrocnemius/plantaris), respectively. B and D, Bar graphs represent means ± SEM of n = 9 to 11; data were normalized to actin, and data from control mice were arbitrarily set at 1.0 AU. *$P < .05$ compared with time-matched control values.

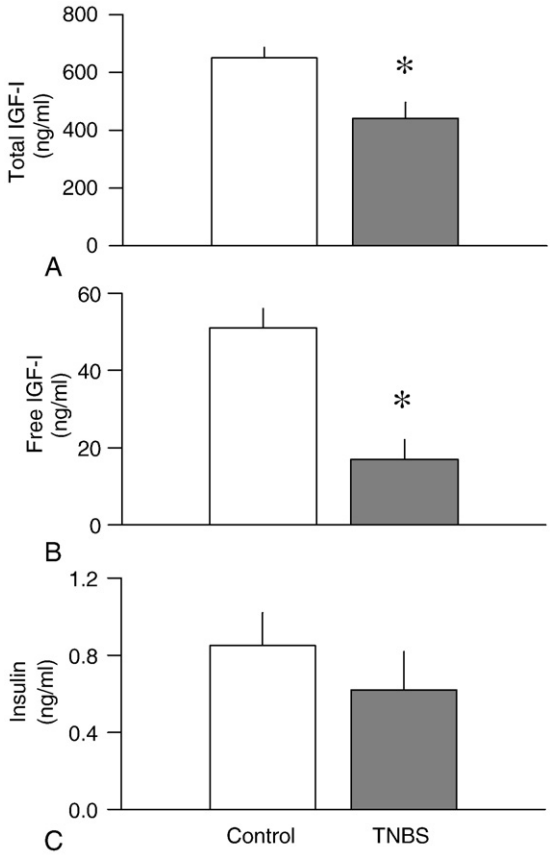

Fig. 4. Effect of TNBS-induced colitis on the plasma concentration of total and free IGF-I, and insulin (A-C, respectively). Bar graphs represent means ± SEM of n = 9 to 11. *$P < .05$ compared with time-matched control values.

control animals indicated no significant difference ($P > .10$) in either the extent of phosphorylation (eg, activation) or total amount of 4E-BP1 or S6K1 (data not shown).

The rate of protein degradation in the plantaris muscle was determined in vitro and shown to be increased 45% ($P < .05$) in mice with colitis compared with time-matched control values (Fig. 1A). In addition, in vitro–determined 26S proteasome activity of gastrocnemius was increased 85% ($P < .05$) in muscle from TNBS-treated mice (Fig. 1B). The 20S proteasome activity also tended to be increased ($P = .08$) in TNBS-treated mice (Fig. 1C).

3.3. Muscle mRNA expression of MuRF1, atrogin-1, and E3α1

The E3 ligases MuRF1 and atrogin-1 are important regulators of protein degradation in muscle; and therefore, we examined the mRNA levels of these enzymes. The MuRF1 mRNA content of skeletal muscle was increased approximately 100% ($P < .05$) in TNBS-treated mice compared with control animals (Fig. 2A, B). There was a similar increase ($P < .05$) in atrogin-1 mRNA content of muscle from mice with colitis (Fig. 2A, C). However, the E3α1 mRNA content did not differ between TNBS-treated and control mice (Fig. 2A, D).

3.4. IGF-I system

We next systematically examined the level of IGF-I in the plasma and IGF-I mRNA content in liver and skeletal muscle. We found that the liver IGF-I mRNA content was decreased 55% ($P < .05$) in the TNBS-treated mice compared with control values (Fig. 3A, B). In contrast, the muscle IGF-I mRNA content did not differ between groups (Fig. 3C, D).

The colitis-induced reduction in the liver IGF-I mRNA was consistent with the 40% reduction ($P < .05$) in the plasma total IGF-I concentration (Fig. 4A). The "free" or easily dissociable IGF-I in the circulation demonstrated a 70% reduction ($P < .05$) in mice with colitis (Fig. 4B). The plasma insulin concentration did not differ between TNBS-treated and control mice (Fig. 4C).

The TNBS-induced colitis also altered the mRNA content for several of the IGFBPs. Insulin-like growth factor binding protein–3 binds most of the plasma IGF-I [3], whereas elevations in plasma IGFBP-1 can decrease muscle protein synthesis [32]. Therefore, the levels of IGFBP-1 and IGFBP-

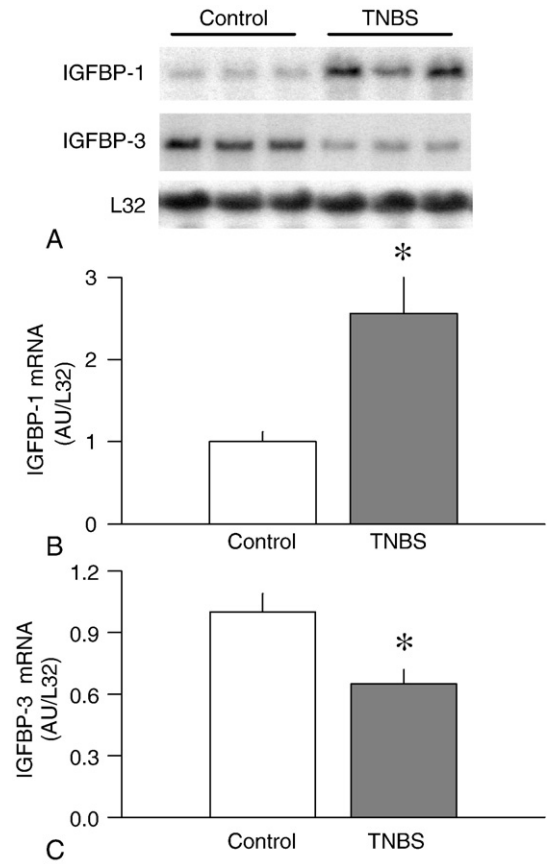

Fig. 5. Effect of TNBS-induced colitis on IGFBP-1 and IGFBP-3 mRNA content in liver. A, Representative autoradiographs of IGFBP-1 and IGFBP-3 mRNA in liver. B and C, Bar graphs represent means ± SEM of n = 9 to 11, where data were normalized to mouse ribosomal protein L32 mRNA signal and expressed as AU/L32. Data from control mice were arbitrarily set at 1.0 AU. *$P < .05$ compared with time-matched control values.

Table 2
Insulin-like growth factor binding protein mRNA in liver and muscle from control and TNBS-treated mice

		Control	TNBS
Liver	IGFBP-2	1.00 ± 0.05	1.11 ± 0.12
	IGFBP-4	1.00 ± 0.08	0.89 ± 0.14
	IGFBP-5	1.00 ± 0.09	0.99 ± 0.07
	IGFBP-6	1.00 ± 0.08	1.17 ± 0.13
	ALS	1.00 ± 0.09	0.87 ± 0.15
Muscle	IGFBP-4	1.00 ± 0.11	0.98 ± 0.08
	IGFBP-5	1.00 ± 0.08	1.07 ± 0.11
	IGFBP-6	1.00 ± 0.07	1.03 ± 0.08

Values are means ± SEM of n = 8. Data were normalized to mouse ribosomal protein L32 mRNA signal, and data from control mice were arbitrarily set at 1.0 AU. There are no statistically significant ($P > .1$) differences between TNBS-treated and time-matched control values for any IGFBP. The mRNAs for IGFBP-1 and -2 were not detectable in skeletal muscle by the RPA methods used in this study.

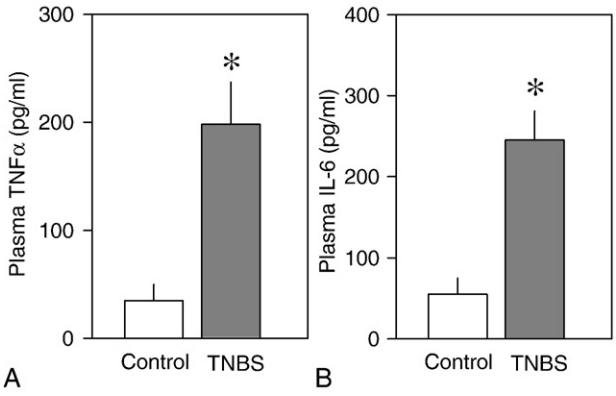

Fig. 7. Effect of TNBS-induced colitis on the plasma concentration of TNF-α and IL-6. Bar graphs in A (TNF-α) and B (IL-6) represent means ± SEM of n = 9 to 11. *$P < .05$ compared with time-matched control values.

3 mRNA in liver—their primary site of synthesis—as well as in skeletal muscle were determined because they might affect local IGF-I bioactivity. In liver, TNBS increased IGFBP-1 by 100% ($P < .05$) and decreased IGFBP-3 mRNA by 40% ($P < .05$) compared with control values (Fig. 5). In contrast, the mRNA content of the other detectable IGF-I binding proteins in liver (eg, IGFBP-2, -4, -5, and -6 and ALS) and in skeletal muscle (eg, IGFBP-3, -4, and -5) did not differ between groups (Table 2).

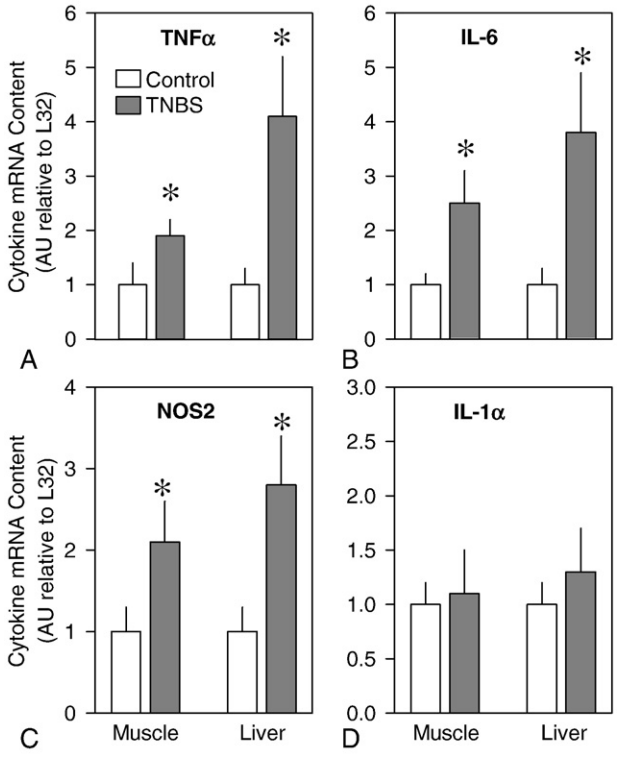

Fig. 6. Effect of TNBS-induced colitis on muscle and liver mRNA content for TNF-α, IL-6, NOS2, and IL-1α (A-D, respectively). Bar graphs represent means ± SEM of n = 9 to 11, where data were normalized to mouse ribosomal protein L32 mRNA signal and data from control mice were arbitrarily set at 1.0 AU. *$P < .05$ compared with time-matched control values for the same tissue.

3.5. Blood and tissue content of inflammatory cytokines

The TNF-α mRNA content was increased approximately 100% ($P < .05$) in muscle and almost 400% ($P < .05$) in liver (Fig. 6A), whereas IL-6 mRNA levels were increased approximately 250% ($P < .05$) in muscle and nearly 400% ($P < .05$) in liver (Fig. 6B). Likewise, NOS2 mRNA levels were elevated approximately 200% to 250% ($P < .05$) in both muscle and liver of mice with colitis (Fig. 6C). In contrast, the IL-1α mRNA content of both muscle and liver did not differ between groups (Fig. 6D). Finally, the plasma concentrations of TNF-α (Fig. 7A) and IL-6 (Fig. 7B) were also elevated ($P < .05$) in mice with colitis compared with vehicle-treated control mice.

4. Discussion

Trinitrobenzene sulfonic acid–induced colitis decreased both skeletal muscle mass and protein concentration over the duration of the 10-day experimental protocol. Muscle protein content represents the balance between protein synthesis and degradation, and not all catabolic insults affect both sides of the protein balance equation in the same manner. Hence, it was important to characterize both rates of synthesis and breakdown in the murine TNBS model of colitis. No significant difference in the in vivo–determined rate of protein synthesis was detected in muscle of control and TNBS-treated mice; and this finding was supported by the comparable phosphorylation status of both 4E-BP1 and S6K1, which are important regulators of mRNA translation. Although our data on protein synthesis and mammalian target of rapamycin activity are internally consistent, they contrast with previous reports where muscle protein synthesis was either reduced [19] or even increased [20] in response to intestinal inflammation. The reason for these highly diver-

gent results is unclear but may be related to use of different experimental models of IBD. Alternatively, because synthesis was only determined at a single time point, we cannot exclude the possibility that a TNBS-induced alteration in muscle protein synthesis occurred at an earlier time point but was transient in nature. Finally, the comparable rates of muscle protein synthesis between groups suggest that the transient reduction in food intake seen in the TNBS-treated mice did not have a sustained effect on this component of the protein balance equation.

An increased rate of muscle protein breakdown is often observed in catabolic states, and the activation of the Ub-proteasome pathway appears to be largely responsible [21]. In the current study, protein breakdown in incubated plantaris was increased in TNBS-treated mice. Likewise, in vitro–determined proteasome activity was increased in muscle from mice colitis. Finally, the mRNA content for 2 muscle-specific E3 ligases atrogin-1 and MuRF1 (but not the more ubiquitously expressed E3α1) were shown to be increased in TNBS-treated mice. Although atrogin-1 and MuRF1 protein content was not determined in our study, the TNBS-induced increase in atrogene mRNA expression is consistent with the up-regulation of muscle atrogin-1 and MuRF1 mRNA in response to other catabolic disease states with muscle wasting, including sepsis, burn, diabetes, and denervation [23-26,28]. Moreover, the atrophic response to denervation was attenuated in either atrogin-1 or MuRF1 null mice [23], clearly demonstrating the central role of these proteins in muscle wasting. Collectively, our data indicate that the skeletal muscle atrophy detected in TNBS-treated mice appears to be predominantly due to an accelerated rate of protein breakdown mediated by the up-regulation of the Ub-proteasome proteolytic pathway.

Insulin-like growth factor–I, via its ability to stimulate protein synthesis and inhibit proteolysis in skeletal muscle, has a central role in maintaining muscle mass [8]; and its effects on muscle metabolism are mediated by not only endocrine but paracrine/autocrine mechanisms [6]. Other catabolic conditions are associated with a reduction in both the circulating concentration of total IGF-I, derived primarily from the liver, and IGF-I synthesized within skeletal muscle per se [32,33,45]. Previous studies in various rodent models of colitis have reported a reduction in the circulating and/or hepatic synthesis of IGF-I [4,12], a response comparable to that seen in IBD patients [1,17,18]. This IBD-induced fall in IGF-I results from the development of GH resistance [46] resulting from the overproduction of various inflammatory cytokines, particularly TNF-α and IL-6 [4,11,12,18,47], a mechanism that is also present in several other catabolic conditions [13]. The GH resistance and decreased plasma IGF-I in children with IBD appear to be largely responsible for the observed growth failure. The current study confirms the previously reported colitis-induced reduction in blood-borne IGF-I [4,11,12,18]. However, our data also extend these observations by demonstrating that colitis does not decrease IGF-I mRNA content in skeletal muscle. This finding suggests that colitis may be somewhat unique compared with other catabolic conditions in that it produces muscle wasting primarily via the loss of the classic endocrine actions of IGF-I as opposed to the local muscle-specific production of the hormone.

In addition to determining total IGF-I, we also assessed the concentration of "free" IGF-I, that is, the amount of IGF-I that is not bound to one of the many IGFBPs and that is believed to represent the physiologically active pool of the hormone [48]. The concentration of free IGF-I is also reduced in other catabolic conditions, and this reduction is proportional to the reduction in total IGF-I [49-51]. However, in the current study, colitis produced a disproportionate fall in free IGF-I that may have resulted from concomitant changes in the various IGFBPs, as these proteins function to alter IGF-I half-life and bioavailability. Of the 6 high-affinity binding proteins, IGFBP-3 is the most predominant and binds the majority of the IGF-I in blood [14].

Insulin-like growth factor–I and IGFBP-3 form a ternary complex with ALS that slows the clearance of IGF-I from the circulation. Many cell types, including hepatocytes, produce IGFBP-3, whereas ALS is produced almost exclusively in the liver under the control of GH [52]. Trinitrobenzene sulfonic acid–induced colitis decreased the hepatic mRNA content of IGFBP-3 and ALS, although the latter change did not achieve statistical significance. Although not directly determined in our study, such changes in IGFBP mRNA would be expected to lower the circulating concentration of both proteins. In addition, catabolic conditions are often associated with extensive proteolytic cleavage of IGFBP-3 [53] that would be expected to further exacerbate the decreased hepatic synthesis of this binding protein. In contrast, IGFBP-1 is acutely up-regulated by infection or catabolic insults [9]; and elevated IGFBP-1 decreases both the plasma concentration of free IGF-I and muscle protein synthesis [15,16]. However, because only a small fraction of total IGF-I is bound to IGFBP-1, the colitis-induced decrease in IGFBP-3 should more than compensate for the elevation in IGFBP-1 and is likely responsible for the disproportionate reduction in free IGF-I. The down-regulation of IGFBP-3 and up-regulation of IGFBP-1 can be coordinately controlled by the same inflammatory cytokines that decrease hepatic IGF-I synthesis and reduce muscle mass [54-58]. One caveat of our study is that only the mRNA content for the various IGFBPs was determined in muscle because of the limited amount of available muscle. Therefore, we cannot exclude the possibility that the TNBS-induced change in the tissue mRNA and protein expression for IGFBP-1 and -3 are not coordinately regulated.

The current study also quantifies the mRNA content of the other IGFBPs in the liver and muscle, which have not been previously reported in colitis. Serum levels of IGFBP-2 have been reported to be higher in human patients experiencing a relapse of Crohn disease compared with healthy controls [18]. However, we did not detect a

significant change in IGFBP-2 mRNA content in liver of mice administered TNBS. Similarly, we also failed to detect significant changes in IGFBP-4, -5, or -6 in either liver or skeletal muscle. The lack of a change in muscle IGFBP-5 was unexpected given that muscle atrophy resulting from disuse or denervation is associated with a marked increase in this IGFBP [59]. Moreover, the lack of change in muscle IGFBP-4 was not anticipated because bacterial infection, which also increases proinflammatory cytokines, has been reported to decrease muscle IGFBP-4 [60]. Our data suggest that, compared with other catabolic conditions, colitis produces a somewhat unique pattern of IGFBP mRNA expression in muscle; and the lack of change in muscle IGF-I, IGFBP-4, and IGFBP-5 in this condition suggests a different mechanism of action.

The growth failure of IBD of various etiologies is associated with elevated blood concentrations of TNF-α and IL-6, and at least part of this elevation may be attributable to up-regulated cytokine production by the inflamed section of gut [4,11,12]. Both of these cytokines decrease IGF-I and have the ability to impair linear growth and decrease LBM [61,62], whereas neutralization of either TNF-α or IL-6 in part restores IGF-I and growth [4,11,12,18]. We extended these observations by showing that the mRNA content for both TNF-α and IL-6 (but not IL-1α) was increased in liver and skeletal muscle in TNBS-treated mice. Elevation in TNF-α and IL-6 was associated with reduced circulating IGF-I, elevated MuRF1 and atrogin-1 in skeletal muscle, and the erosion of LBM in mice with colitis. However, we cannot differentiate between an endocrine or paracrine/autocrine mechanism for these cytokines because TNF-α and IL-6 were increased in liver (the primary source for the elevation in the plasma) as well as in muscle. Finally, gut inflammation is also associated with overproduction of NO via activation of NOS2 in intestinal epithelial cells [63]; and the sustained elevation of NO is likely to be partially responsible for the increased gut permeability and pathology in IBD [64]. However, no data are available on colitis-induced NO production in skeletal muscle; and this is important because enhanced NO production can lead to muscle atrophy [39]. In the present study, colitis increased NOS2 mRNA in both liver and muscle. Regardless of their source, it is noteworthy that the elevated levels of TNF-α, IL-6, and NO failed to decrease muscle protein synthesis in TNBS-treated mice. This lack of response differs from the decreased muscle protein synthesis seen in other catabolic states characterized by elevated inflammatory cytokines (eg, sepsis) or that results from elevated cytokine levels per se [41,44,65]. The mechanism for this discordant response is not known.

In conclusion, the present study demonstrates that TNBS-induced colitis produces muscle atrophy most likely by increasing protein breakdown as opposed to changing protein synthesis. Moreover, the stimulation of protein degradation appears to be mediated via activation of the Ub-proteasome pathway and enhanced expression of atrogin-1 and MuRF1. The increased protein degradation is associated with a reduction in circulating (but not muscle) IGF-I as well as increased muscle and circulating TNF-α, IL-6, and NO. Hence, interfering with the activation of the Ub-proteasome pathway may prove to be beneficial in ameliorating the debilitating effects of growth retardation and the impairment in muscle protein accretion in patients with IBD.

Acknowledgment

Support: National Institute of Health grants GM-55639 (RNC), GM-38032 (CHL), and T32-GM64332 (FP), and The Crohn's and Colitis Foundation of America from the Litwin Foundation (RNC). We thank Jay Nystrom and Anne Pruznak for their expert technical assistance.

References

[1] Griffiths AM, Nguyen P, Smith C, et al. Growth and clinical course of children with Crohn's disease. Gut 1993;34:939-43.
[2] Motil KJ, Grand RJ, vis-Kraft L, et al. Growth failure in children with inflammatory bowel disease: a prospective study. Gastroenterology 1993;105:681-91.
[3] Ballinger A. Fundamental mechanisms of growth failure in inflammatory bowel disease. Horm Res 2002;58(Suppl 1):7-10.
[4] Ballinger AB, Azooz O, El-Haj T, et al. Growth failure occurs through a decrease in insulin-like growth factor 1 which is independent of undernutrition in a rat model of colitis. Gut 2000;46:694-700.
[5] Shamir R, Phillip M, Levine A. Growth retardation in pediatric Crohn's disease: pathogenesis and interventions. Inflamm Bowel Dis 2007;13:620-8.
[6] Le RD, Bondy C, Yakar S, et al. The somatomedin hypothesis: 2001. Endocr Rev 2001;22:53-74.
[7] Olney RC. Regulation of bone mass by growth hormone. Med Pediatr Oncol 2003;41:228-34.
[8] Clemmons DR. Role of IGF-I in skeletal muscle mass maintenance. Trends Endocrinol Metab 2009;20:349-56.
[9] Frost RA, Lang CH. Alteration of somatotropic function by proinflammatory cytokines. J Anim Sci 2004;82(E-Suppl):E100-9.
[10] Denson LA, Held MA, Menon RK, et al. Interleukin-6 inhibits hepatic growth hormone signaling via upregulation of Cis and Socs-3. Am J Physiol Gastrointest Liver Physiol 2003;284:G646-54.
[11] DiFedele LM, He J, Bonkowski EL, et al. Tumor necrosis factor alpha blockade restores growth hormone signaling in murine colitis. Gastroenterology 2005;128:1278-91.
[12] Sawczenko A, Azooz O, Paraszczuk J, et al. Intestinal inflammation-induced growth retardation acts through IL-6 in rats and depends on the −174 IL-6 G/C polymorphism in children. Proc Natl Acad Sci U S A 2005;102:13260-5.
[13] Lang CH, Hong-Brown L, Frost RA. Cytokine inhibition of JAK-STAT signaling: a new mechanism of growth hormone resistance. Pediatr Nephrol 2005;20:306-12.
[14] Firth SM, Baxter RC. Cellular actions of the insulin-like growth factor binding proteins. Endocr Rev 2002;23:824-54.
[15] Frost RA, Lang CH. Differential effects of insulin-like growth factor I (IGF-I) and IGF- binding protein–1 on protein metabolism in human skeletal muscle cells. Endocrinology 1999;140:3962-70.
[16] Lang CH, Vary TC, Frost RA. Acute in vivo elevation of insulin-like growth factor (IGF) binding protein–1 decreases plasma free IGF-I and muscle protein synthesis. Endocrinology 2003;144:3922-33.
[17] Eivindson M, Gronbaek H, Flyvbjerg A, et al. The insulin-like growth factor (IGF)–system in active ulcerative colitis and Crohn's disease:

relations to disease activity and corticosteroid treatment. Growth Horm IGF Res 2007;17:33-40.
[18] Eivindson M, Gronbaek H, Skogstrand K, et al. The insulin-like growth factor (IGF) system and its relation to infliximab treatment in adult patients with Crohn's disease. Scand J Gastroenterol 2007;42: 464-70.
[19] Mercier S, Breuille D, Mosoni L, et al. Chronic inflammation alters protein metabolism in several organs of adult rats. J Nutr 2002;132: 1921-8.
[20] El YM, Breuille D, Papet I, et al. Increased tissue protein synthesis during spontaneous inflammatory bowel disease in HLA-B27 rats. Clin Sci (Lond) 2003;105:437-46.
[21] Lecker SH, Solomon V, Mitch WE, et al. Muscle protein breakdown and the critical role of the ubiquitin-proteasome pathway in normal and disease states. J Nutr 1999;129:227S-37S.
[22] Roos-Mattjus P, Sistonen L. The ubiquitin-proteasome pathway. Ann Med 2004;36:285-95.
[23] Bodine SC, Latres E, Baumhueter S, et al. Identification of ubiquitin ligases required for skeletal muscle atrophy. Science 2001;294: 1704-8.
[24] Frost RA, Nystrom GJ, Jefferson LS, et al. Hormone, cytokine, and nutritional regulation of sepsis-induced increases in atrogin-1 and MuRF1 in skeletal muscle. Am J Physiol Endocrinol Metab 2007;292: E501-12.
[25] Krawiec BJ, Nystrom GJ, Frost RA, et al. AMP-activated protein kinase agonists increase mRNA content of the muscle-specific ubiquitin ligases MAFbx and MuRF1 in C2C12 cells. Am J Physiol Endocrinol Metab 2007;292:E1555-67.
[26] Li HH, Kedar V, Zhang C, et al. Atrogin-1/muscle atrophy F-box inhibits calcineurin- dependent cardiac hypertrophy by participating in an SCF ubiquitin ligase complex. J Clin Invest 2004;114:1058-71.
[27] Nystrom G, Pruznak A, Huber D, et al. Local insulin-like growth factor I prevents sepsis- induced muscle atrophy. Metabolism 2009;58: 787-97.
[28] Sacheck JM, Ohtsuka A, McLary SC, et al. IGF-I stimulates muscle growth by suppressing protein breakdown and expression of atrophy-related ubiquitin ligases, atrogin-1 and MuRF1. Am J Physiol Endocrinol Metab 2004;287:E591-601.
[29] Morris GP, Beck PL, Herridge MS, et al. Hapten-induced model of chronic inflammation and ulceration in the rat colon. Gastroenterology 1989;96:795-803.
[30] Zhang XJ, Cortiella J, Doyle D, et al. Ketamine anesthesia causes greater muscle catabolism in rabbits than does propofol. J Nutr Biochem 1997;8:133-9.
[31] Garlick PJ, McNurlan MA, Preedy VR. A rapid and convenient technique for measuring the rate of protein synthesis in tissues by injection of [3H]phenylalanine. Biochem J 1980;192:719-23.
[32] Lang CH, Frost RA. Differential effect of sepsis on ability of leucine and IGF-I to stimulate muscle translation initiation. Am J Physiol Endocrinol Metab 2004;287:E721-30.
[33] Lang CH, Frost RA. Endotoxin disrupts the leucine-signaling pathway involving phosphorylation of mTOR, 4E-BP1, and S6K1 in skeletal muscle. J Cell Physiol 2005;203:144-55.
[34] Vary TC, Frost RA, Lang CH. Acute alcohol intoxication increases atrogin-1 and MuRF1 mRNA without increasing proteolysis in skeletal muscle. Am J Physiol Regul Integr Comp Physiol 2008;294: R1777-89.
[35] Waalkes TP, Udenfriend S. A fluorometric method for the estimation of tyrosine in plasma and tissues. J Lab Clin Med 1957;50:733-6.
[36] Solomon V, Goldberg AL. Importance of the ATP-ubiquitin-proteasome pathway in the degradation of soluble and myofibrillar proteins in rabbit muscle extracts. J Biol Chem 1996;271:26690-7.
[37] Wang X, Hu Z, Hu J, et al. Insulin resistance accelerates muscle protein degradation: activation of the ubiquitin-proteasome pathway by defects in muscle cell signaling. Endocrinology 2006;147:4160-8.
[38] Frost RA, Nystrom GJ, Lang CH. Lipopolysaccharide regulates proinflammatory cytokine expression in mouse myoblasts and skeletal muscle. Am J Physiol Regul Integr Comp Physiol 2002; 283:R698-709.
[39] Frost RA, Nystrom GJ, Lang CH. Lipopolysaccharide stimulates nitric oxide synthase–2 expression in murine skeletal muscle and C(2)C(12) myoblasts via Toll-like receptor-4 and c- Jun NH(2)-terminal kinase pathways. Am J Physiol Cell Physiol 2004;287:C1605-15.
[40] Lang CH, Pruznak AM, Nystrom GJ, et al. Alcohol-induced decrease in muscle protein synthesis associated with increased binding of mTOR and raptor: comparable effects in young and mature rats. Nutr Metab (Lond) 2009;6:4.
[41] Lang CH, Frost RA, Nairn AC, et al. TNF-alpha impairs heart and skeletal muscle protein synthesis by altering translation initiation. Am J Physiol Endocrinol Metab 2002;282:E336-47.
[42] Lang CH, Frost RA. Glucocorticoids and TNFalpha interact cooperatively to mediate sepsis-induced leucine resistance in skeletal muscle. Mol Med 2006;12:291-9.
[43] Lang CH, Frost RA. Sepsis-induced suppression of skeletal muscle translation initiation mediated by tumor necrosis factor alpha. Metabolism 2007;56:49-57.
[44] Lang CH, Frost RA, Vary TC. Regulation of muscle protein synthesis during sepsis and inflammation. Am J Physiol Endocrinol Metab 2007;293:E453-9.
[45] Pruznak AM, Hong-Brown L, Lantry R, et al. Skeletal and cardiac myopathy in HIV-1 transgenic rats. Am J Physiol Endocrinol Metab 2008;295:E964-73.
[46] Theiss AL, Fruchtman S, Lund PK. Growth factors in inflammatory bowel disease: the actions and interactions of growth hormone and insulin-like growth factor–I. Inflamm Bowel Dis 2004;10: 871-80.
[47] Mitsuyama K, Sata M, Rose-John S. Interleukin-6 trans-signaling in inflammatory bowel disease. Cytokine Growth Factor Rev 2006;17: 451-61.
[48] Frystyk J. Utility of free IGF-I measurements. Pituitary 2007;10:181-7.
[49] Bereket A, Lang CH, Blethen SL, et al. Growth hormone treatment in growth retarded children with end stage renal failure: effect on free/dissociable IGF-I levels. J Pediatr Endocrinol Metab 1997;10: 197-202.
[50] Co Ng LL, Lang CH, Bereket A, et al. Effect of hyperthyroidism on insulin-like growth factor–I (IGF-I) and IGF-binding proteins in adolescent children. J Pediatr Endocrinol Metab 2000;13:1073-80.
[51] Lang CH, Liu X, Nystrom G, et al. Acute effects of growth hormone in alcohol-fed rats. Alcohol Alcohol 2000;35:148-58.
[52] Laursen T, Flyvbjerg A, Jorgensen JO, et al. Stimulation of the 150-kilodalton insulin-like growth factor-binding protein–3 ternary complex by continuous and pulsatile patterns of growth hormone (GH) administration in GH-deficient patients. J Clin Endocrinol Metab 2000;85:4310-4.
[53] Belizon A, Kirman I, Balik E, et al. Major surgical trauma induces proteolysis of insulin-like growth factor binding protein–3 in transgenic mice and is associated with a rapid increase in circulating levels of matrix metalloproteinase-9. Surg Endosc 2007;21:653-8.
[54] Barreca A, Ketelslegers JM, Arvigo M, et al. Decreased acid-labile subunit (ALS) levels by endotoxin in vivo and by interleukin-1beta in vitro. Growth Horm IGF Res 1998;8:217-23.
[55] Benbassat CA, Lazarus DD, Cichy SB, et al. Interleukin-1 alpha (IL-1 alpha) and tumor necrosis factor alpha (TNF alpha) regulate insulin-like growth factor binding protein–1 (IGFBP-1) levels and mRNA abundance in vivo and in vitro. Horm Metab Res 1999;31:209-15.
[56] Delhanty PJ. Interleukin-1 beta suppresses growth hormone-induced acid-labile subunit mRNA levels and secretion in primary hepatocytes. Biochem Biophys Res Commun 1998;243:269-72.
[57] Fan J, Char D, Bagby GJ, et al. Regulation of insulin-like growth factor–I (IGF-I) and IGF- binding proteins by tumor necrosis factor. Am J Physiol 1995;269:R1204-12.
[58] Fan J, Wojnar MM, Theodorakis M, et al. Regulation of insulin-like growth factor (IGF)–I mRNA and peptide and IGF-binding proteins by interleukin-1. Am J Physiol 1996;270:R621-9.

[59] Bayol S, Loughna PT, Brownson C. Phenotypic expression of IGF binding protein transcripts in muscle, in vitro and in vivo. Biochem Biophys Res Commun 2000;273:282-6.

[60] Lang CH, Krawiec BJ, Huber D, et al. Sepsis and inflammatory insults downregulate IGFBP-5, but not IGFBP-4, in skeletal muscle via a TNF-dependent mechanism. Am J Physiol Regul Integr Comp Physiol 2006;290:R963-72.

[61] De BF, Alonzi T, Moretta A, et al. Interleukin 6 causes growth impairment in transgenic mice through a decrease in insulin-like growth factor–I. A model for stunted growth in children with chronic inflammation. J Clin Invest 1997;99:643-50.

[62] Martensson K, Chrysis D, Savendahl L. Interleukin-1beta and TNF-alpha act in synergy to inhibit longitudinal growth in fetal rat metatarsal bones. J Bone Miner Res 2004;19:1805-12.

[63] Wu F, Chakravarti S. Differential expression of inflammatory and fibrogenic genes and their regulation by NF-kappaB inhibition in a mouse model of chronic colitis. J Immunol 2007;179:6988-7000.

[64] Kubes P, McCafferty DM. Nitric oxide and intestinal inflammation. Am J Med 2000;109:150-8.

[65] Janssen SP, Gayan-Ramirez G, Van den BA, et al. Interleukin-6 causes myocardial failure and skeletal muscle atrophy in rats. Circulation 2005;111:996-1005.